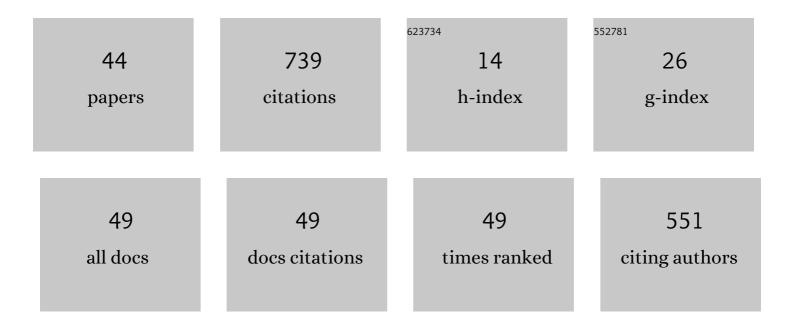
Annelies Malfliet

List of Publications by Year in descending order

Source: https://exaly.com/author-pdf/8531442/publications.pdf Version: 2024-02-01



#	Article	IF	CITATIONS
1	Capillary Interaction Between Micron-Sized Ce2O3 Inclusions at the Ar Gas/Liquid Steel Interface. Metallurgical and Materials Transactions B: Process Metallurgy and Materials Processing Science, 2022, 53, 1775-1791.	2.1	5
2	Role of Interfacial Properties in the Evolution of Non-metallic Inclusions in Liquid Steel. ISIJ International, 2022, 62, 1573-1585.	1.4	5
3	Kinetic Aspects of Aluminum Oxide Dissolution in Molten BOF Slag. Metallurgical and Materials Transactions B: Process Metallurgy and Materials Processing Science, 2021, 52, 1614-1625.	2.1	3
4	In Situ Electrical Conductivity Measurement by Using Confocal Scanning Laser Microscopy. Metallurgical and Materials Transactions B: Process Metallurgy and Materials Processing Science, 2021, 52, 2563-2572.	2.1	7
5	A First-Principles Tool to Discover New Pyrometallurgical Refining Options. Jom, 2021, 73, 2900-2910.	1.9	1
6	Characterization of antimony-containing metallurgical residues for antimony recovery. Journal of Cleaner Production, 2021, 327, 129491.	9.3	7
7	HDDR treatment of Ce-substituted Nd2Fe14B-based permanent magnetÂalloys - phase structure evolution, intergranular processes and magnetic property development. Journal of Alloys and Compounds, 2020, 814, 152215.	5.5	15
8	Genesis of As-Pb-Rich Supergene Mineralization: The Tazalaght and Agoujgal Cu Deposits (Moroccan) Tj ETQq0 0	0,rggBT /O	verlock 10 T
9	A Study of the Occurrence of Selected Rare-Earth Elements in Neutralized–Leached Bauxite Residue and Comparison with Untreated Bauxite Residue. Journal of Sustainable Metallurgy, 2019, 5, 57-68.	2.3	14
10	Influence of Al2O3 Level in CaO-SiO2-MgO-Al2O3 Refining Slags on Slag/Magnesia-Doloma Refractory Interactions. Metallurgical and Materials Transactions B: Process Metallurgy and Materials Processing Science, 2019, 50, 1822-1829.	2.1	6
11	Dissolution Behavior and Phase Evolution During Aluminum Oxide Dissolution in BOF Slag. Metallurgical and Materials Transactions B: Process Metallurgy and Materials Processing Science, 2019, 50, 1782-1790.	2.1	9
	Preface to the 5th International Slag Valorisation Symposium. From Eurodamentals to Applications		

12	Journal of Sustainable Metallurgy, 2018, 4, 1-2.	2.3	3
13	Inorganic polymers made of fayalite slag: On the microstructure and behavior of Fe. Journal of the American Ceramic Society, 2018, 101, 2245-2257.	3.8	43
14	Degradation mechanisms of alumina-chromia refractories for secondary copper smelter linings. Corrosion Science, 2018, 136, 409-417.	6.6	41
15	Rheological Transitions of the Solid-Bearing Slag During Cooling Process. Metallurgical and Materials Transactions B: Process Metallurgy and Materials Processing Science, 2018, 49, 2649-2657.	2.1	4
16	Aluminum Deoxidation Equilibrium of Fe-Ni Alloy at 1773ÂK and 1873ÂK. Metallurgical and Materials Transactions B: Process Metallurgy and Materials Processing Science, 2018, 49, 2389-2399.	2.1	8
17	Rare Earth Element Phases in Bauxite Residue. Minerals (Basel, Switzerland), 2018, 8, 77.	2.0	58
18	Effect of Surfactant Te on the Formation of MnS Inclusions in Steel. Metallurgical and Materials Transactions B: Process Metallurgy and Materials Processing Science, 2017, 48, 2447-2458.	2.1	31

ANNELIES MALFLIET

#	Article	IF	CITATIONS
19	Electrochemical Extraction of Rare Earth Metals in Molten Fluorides: Conversion of Rare Earth Oxides into Rare Earth Fluorides Using Fluoride Additives. Journal of Sustainable Metallurgy, 2017, 3, 627-637.	2.3	38
20	Effect of Alumina Morphology on the Clustering of Alumina Inclusions in Molten Iron. ISIJ International, 2016, 56, 926-935.	1.4	34
21	Effect of Impurity Te on the Morphology of Alumina Particles in Molten Iron. ISIJ International, 2016, 56, 1529-1536.	1.4	4
22	Influence of FeO/SiO ₂ and CaO/SiO ₂ Ratios in Iron‣aturated ZnOâ€Rich Fayalite Slags on the Corrosion of MgO. Journal of the American Ceramic Society, 2016, 99, 3754-3760.	3.8	20
23	Thermodynamic assessment of the Nd2O3-CaO-SiO2 ternary system. Calphad: Computer Coupling of Phase Diagrams and Thermochemistry, 2016, 55, 157-164.	1.6	6
24	Spinel saturation of a PbO based slag as a method to mitigate the chemical degradation of magnesia-chromite bricks. Journal of the European Ceramic Society, 2016, 36, 4291-4299.	5.7	5
25	Effect of surfactant Te on the behavior of alumina inclusions at advancing solid-liquid interfaces of liquid steel. Acta Materialia, 2016, 120, 443-452.	7.9	10
26	Study of Phase Relations of ZnO-Containing Fayalite Slag Under Fe Saturation. Metallurgical and Materials Transactions B: Process Metallurgy and Materials Processing Science, 2016, 47, 2820-2829.	2.1	4
27	Slag Valorisation as a Contribution to Zero-Waste Metallurgy. Journal of Sustainable Metallurgy, 2016, 2, 1-2.	2.3	5
28	Phase Relations of the CaO-SiO2-Nd2O3 System and the Implication for Rare Earths Recycling. Metallurgical and Materials Transactions B: Process Metallurgy and Materials Processing Science, 2016, 47, 1736-1744.	2.1	15
29	Effect of ZnO level in secondary copper smelting slags on slag/magnesia-chromite refractory interactions. Journal of the European Ceramic Society, 2016, 36, 1821-1828.	5.7	32
30	Identification of magnesia–chromite refractory degradation mechanisms of secondary copper smelter linings. Journal of the European Ceramic Society, 2016, 36, 2119-2132.	5.7	45
31	Effect of Interfacial Properties on the Characteristics and Clustering of Alumina Inclusions in Molten Iron. ISIJ International, 2015, 55, 1891-1900.	1.4	12
32	Mg-O-Si Chemical Bond Formation in Light Burned Magnesia and Fumed Silica Mixture During Mechanical Activation. InterCeram: International Ceramic Review, 2015, 64, 90-93.	0.2	1
33	The effect of a temperature gradient on the phase formation inside a magnesia–chromite refractory in contact with a non-ferrous PbO–SiO2–MgO slag. Journal of the European Ceramic Society, 2015, 35, 2933-2942.	5.7	12
34	The influence of ZnO in fayalite slag on the degradation of magnesia-chromite refractories during secondary Cu smelting. Journal of the European Ceramic Society, 2015, 35, 2641-2650.	5.7	38
35	The influence of slag compositional changes on the chemical degradation of magnesia-chromite refractories exposed to PbO-based non-ferrous slag saturated in spinel. Journal of the European Ceramic Society, 2015, 35, 347-355.	5.7	19
36	Hydraulic Behavior of Mechanically and Chemically Activated Synthetic Merwinite. Journal of the American Ceramic Society, 2014, 97, 3973-3981.	3.8	13

ANNELIES MALFLIET

#	Article	IF	CITATIONS
37	Stabilisation and Microstructural Modification of Stainless Steel Converter Slag by Addition of an Alumina Rich By-Product. Waste and Biomass Valorization, 2014, 5, 343-353.	3.4	16
38	Degradation mechanisms and use of refractory linings in copper production processes: A critical review. Journal of the European Ceramic Society, 2014, 34, 849-876.	5.7	118
39	Fe3Nb3N precipitates of the Fe3W3C type in Nb stabilized ferritic stainless steel. Journal of Alloys and Compounds, 2011, 509, 9583-9588.	5.5	8
40	Precipitation in Nb-Stabilized Ferritic Stainless Steel Investigated with in-situ and ex-situ Transmission Electron Microscopy. Metallurgical and Materials Transactions A: Physical Metallurgy and Materials Science, 2011, 42, 3333-3343.	2.2	5
41	(Fe, Cr) ₆ Nb ₆ O _x phase of the filled Ti ₂ Ni type with × ± 0.75 in the quaternary Cr–Fe–Nb–O system. International Journal of Materials Research, 2011, 102, 109-116.	0.3	1
42	Precipitation in Fe–15Cr–1Nb alloys after oxygenation. Acta Materialia, 2010, 58, 3832-3841.	7.9	4
43	Effect of Reduction Parameters on the Size and Morphology of the Metallic Particles in Carbothermally Reduced Stainless Steel Dust. Journal of Sustainable Metallurgy, 0, , 1.	2.3	2
44	Capillary Interaction Between Arbitrarily-Shaped Inclusions at the Gas/Steel Interface. Metallurgical and Materials Transactions B: Process Metallurgy and Materials Processing Science, 0, , 1.	2.1	1

4